Output power analyses for the thermodynamic cycles of thermal power plants*

Sun Chen(孙 晨), Cheng Xue-Tao(程雪涛), and Liang Xin-Gang(梁新刚)†

Key Laboratory for Thermal Science and Power Engineering of Ministry of Education, Department of Engineering Mechanics, Tsinghua University, Beijing 100084, *China*

(Received 31 July 2013; revised manuscript received 3 November 2013; published online 1 April 2014)

Thermal power plant is one of the important thermodynamic devices, which is very common in all kinds of power generation systems. In this paper, we use a new concept, entransy loss, as well as exergy destruction, to analyze the single reheating Rankine cycle unit and the single stage steam extraction regenerative Rankine cycle unit in power plants. This is the first time that the concept of entransy loss is applied to the analysis of the power plant Rankine cycles with reheating and steam extraction regeneration. In order to obtain the maximum output power, the operating conditions under variant vapor mass flow rates are optimized numerically, as well as the combustion temperatures and the off-design flow rates of the flue gas. The relationship between the output power and the exergy destruction rate and that between the output power and the entransy loss rate are discussed. It is found that both the minimum exergy destruction rate and the maximum entransy loss rate lead to the maximum output power when the combustion temperature and heat capacity flow rate of the flue gas are prescribed. Unlike the minimum exergy destruction rate, the maximum entransy loss rate is related to the maximum output power when the highest temperature and heat capacity flow rate of the flue gas are not prescribed.

Keywords: thermal power plants, Rankine circle, exergy destruction, entransy loss

PACS: 05.70.−a **DOI:** 10.1088/1674-1056/23/5/050513

1. Introduction

Power plant is one of the most important devices in human life because electric supply directly relates to the economic development and the improvement of the living standards for the people.[1] As thermal power plants are the most used plants in all kinds of power generations, increasing the energy utilization efficiency in thermal power plants has been an important topic for reducing energy consumption.

The basic cycle of a condensing power plant is the Rankine cycle, which absorbs thermal energy from fossil fuel combustion, and converts the thermal energy into mechanical energy by driving turbines. Some kinds of approaches were adopted into Rankine cycles for various demands,[2] including the reheat cycle,[3] the regenerative-reheat Rankine cycle,[4] the two-stage Rankine cycle,[5] etc. The analyses of the power plant cycle are under the category of finite-time thermodynamics, on which many investigations have been done before.[6–9] Generally, the performance of thermal power plants is evaluated by the energetic performance criteria based on the first law of thermodynamics, including the electrical power and the thermal efficiency.[10] According to the heat quantity method, the thermal economic performance of a condensing power station is measured by thermal economic indexes, including the steam consumption rate, the heat consumption rate, the coal consumption rate, and the thermal efficiency.[11] The inlet temperature and pressure of the steam into the turbine can be increased and the turbine exhaust pressure can be reduced to improve the thermal efficiency of the cycle. Reheating and steam extraction regeneration are also used to improve the thermal efficiency.[12]

Based on the second law of thermodynamics, entropy generation is used to evaluate the irreversibility of thermodynamic processes.[12] Researchers have done much work on the analyses of thermodynamic processes by using entropy generation minimization,[13–16] which is also used in power plant analyses. Bejan[17] applied the entropy generation minimization to analyzing and optimizing the processes in power plants. Salamon *et al.*[18] analyzed an example of a power plant to find how the constraints of general entropy principles govern the possible solutions. However, there are exceptions in the entropy generation minimization.[19,20] Klein and Reindl[19] found that minimizing the entropy generation does not always result in the maximum performance of the refrigeration system if the refrigeration capacity is not fixed. Cheng *et al.*[20] revealed that the entropy generation cannot be related to the net work change in the air standard cycle when the heat absorbed is from the combustion of the gas fuel. The exergy method is also used for evaluating the performance of power plants, as a means to optimize the performance and turbine power output.[21–25] The principle of the exergy method is also based on the second law of thermodynamics. As the quality of energy is considered, the exergetic performance not only shows the results of energy conversion, but also reveals the essential reason of energy utilization and the distribution of exergy

*Project supported by the National Natural Science Foundation of China (Grant No. 51376101).

†Corresponding author. E-mail: liangxg@tsinghua.edu.cn

© 2014 Chinese Physical Society and IOP Publishing Ltd

destruction.

On the other hand, entransy,[26] which reflects the potential energy of the heat in an object, was developed and applied to the analyses of finite time thermodynamics recently,[27–29] including some heat-work conversion processes.[30–35] Cheng *et al.*[30–32] proposed the concept of entransy loss that is the difference between the heat entransy flows into and out of the system and is also equal to the sum of the entransy dissipation due to the irreversible heat transfer and the entransy variation due to the work doing processes. For the discussed cases, it was found that the increase of the entransy loss rate leads to the increase of the output power.

The concepts of entransy loss and exergy destruction are used to analyze the thermal power plants with the output power as the focus. In Ref. [34], Wang *et al.* analyzed the ideal Rankine cycle. In this paper, we further investigate the steam power plants with the Rankine cycle in practical applications. Some working cases are discussed, such as the one that deviates from the operating design under varied total heat absorption, the one under variant combustion temperatures, and the one with varied heat capacity flow rates of the flue gas. Reheating and steam extraction regeneration in real power plants are also discussed under the same conditions as well, which are usually adopted in thermal power plants to improve the thermal efficiency of the systems. The conditions and parameters in calculations are consistent with the real power plants.

2. Analyses of the basic Rankine cycles in thermal power plants

2.1. Thermodynamic processes of the basic condensing power plants

The basic Rankine cycle of the thermal power plant is shown in Fig. 1, in which the working fluid is steam.[12] The low pressure saturated water goes through an isentropic compression through a pump, turns into high pressure unsaturated water, and then flows into the boiler to be heated. In most thermal power plants, as shown in Fig. 1(a), the heat absorption can be simplified into three steps. First, the water flows into the economizer, absorbs the heat from the flue gas and is converted into high pressure saturated water. Second, the saturated water is heated and becomes saturated vapor in the tubes of the boiler. Third, the saturated vapor flows into the superheater and changes into superheated vapor under further heating. The high pressure and high temperature superheated vapor goes into the steam turbines and expands isentropically. Then, the waste steam at very low pressure flows into the condenser, and is cooled down to the low pressure saturated water by the cooling water. Finally, the low pressure saturated water returns to the pumps again, and one cycle finishes.

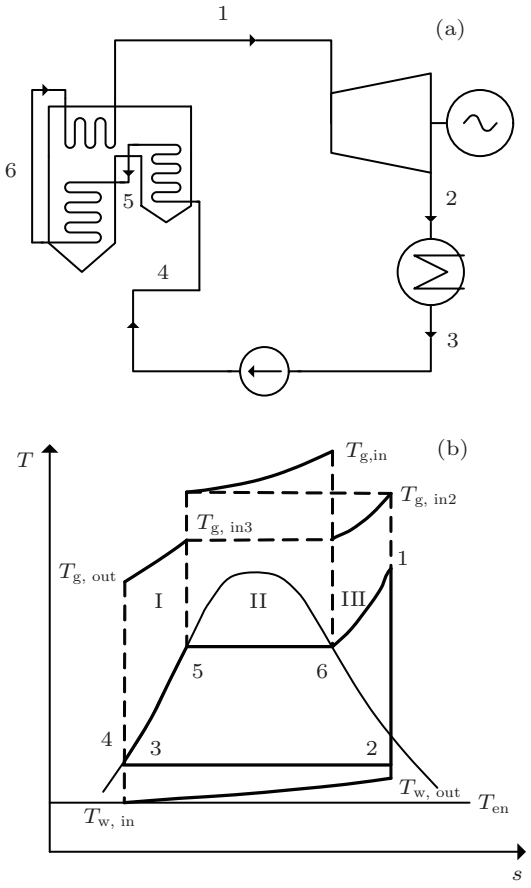


Fig. 1. (a) The flow diagram of the basic Rankine cycle. (b) The T–s diagram of the basic Rankine cycle.

The simplified T–s diagram of the system with the flue gas and cooling water is shown in Fig. 1(b). In practice, the temperature rise of the low pressure saturated water due to compression in the pump can be ignored. Therefore, points 3 and 4 become one point. Process 4–5 is the heating process under constant high pressure in the economizer where the temperature of the flue gas decreases from $T_{g,in3}$ to $T_{g,out}$. $T_{g,in3}$ is the inlet temperature of the economizer flue gas, and $T_{g,out}$ is the outlet temperature of the economizer flue gas. Process 5–6 is the vaporization process under constant pressure and constant temperature, and the flue gas temperature changes from $T_{g,in}$ to $T_{g,in2}$. $T_{g,in}$ is the fuel combustion temperature, and $T_{g,in2}$ is the inlet temperature of the superheater as well. In process 6–1, the water vapor is superheated under constant high pressure in the superheater where the flue gas temperature decreases from $T_{g,in2}$ to $T_{g,in3}$. Process 1–2 is the isentropic expansion process in the turbine. Process 2–3 is the condensation of the used vapor in the condenser where the temperature of the cooling water from the environment increases from $T_{w,in}$ to $T_{w,out}$. $T_{w,in}$ equals the environment temperature T_{en}.

There are many operating parameters that can affect the cycle operation, especially when the operating conditions deviate from the design values of power plants. In the present work, the mass flow rate of the working fluid, m, is optimized

to obtain the maximum output power W. Several conditions are discussed to obtain the relationship between W and m.

We assume that C_g is the heat capacity flow rate of the flue gas, C_w is the heat capacity flow rate of the cooling water, c_v is the specific heat capacity of the high pressure vapor at constant pressure, c_l is the specific heat capacity of the water at constant pressure, r is the latent heat of vaporization at high pressure, and the heat leak to the environment can be ignored. The energy balance equations in sections I–III and the condensation are

$$\begin{aligned} Q_{\rm I} &= mc_l(T_5-T_3) = C_{\rm I,min}\varepsilon_{\rm I}(T_{\rm g,in3}-T_3) \\ &= C_g(T_{\rm g,in3}-T_{\rm g,out}), \quad (1) \\ Q_{\rm II} &= mr = C_g(T_{\rm g,in}-T_{\rm g,in2}), \quad (2) \\ Q_{\rm III} &= mc_v(T_1-T_6) = C_{\rm III,min}\varepsilon_{\rm III}(T_{\rm g,in2}-T_6) \\ &= C_g(T_{\rm g,in2}-T_{\rm g,in3}), \quad (3) \\ Q_c &= C_{\rm c,min}\varepsilon_c(T_2-T_{\rm en}) = C_w(T_{\rm w,out}-T_{\rm en}) \\ &= mT_2(s_2-s_3), \quad (4) \end{aligned}$$

where subscripts I, II, III, and c denote the economizer, boiler tubes, superheater, and the condenser; $C_{\rm I,min}$ is the smaller one between C_g and mc_l, and $C_{\rm I,max}$ is the larger one; $C_{\rm III,min}$ is the smaller one between mc_v and C_g, and $C_{\rm III,max}$ is the larger one; $C_{\rm c,min}$ is the smaller one between the heat capacity flow rate of the working fluid during the condensation and C_w; ε is the heat exchanger effectiveness; and m is the circulation mass flow rate of the cycle. The flow mode of the working fluid in the economizer is designed to be a counter flow. For simplification, the flows in the superheater is considered to be a parallel flow.[1] The heat exchanger effectiveness can be calculated by[36]

$$\varepsilon_{\rm I} = \frac{1-\exp[(-{\rm NTU_I})(1-C_{\rm I,min}/C_{\rm I,max})]}{1-\exp[(-{\rm NTU_I})(1-C_{\rm I,min}/C_{\rm I,max})]C_{\rm I,min}/C_{\rm I,max}}, \quad (5)$$

$$\varepsilon_{\rm III} = \frac{1-\exp[(-{\rm NTU_{III}})(1+C_{\rm III,min}/C_{\rm III,max})]}{1+C_{\rm III,min}/C_{\rm III,max}}, \quad (6)$$

$$\varepsilon_c = 1-\exp(-{\rm NTU_c}). \quad (7)$$

As the heat capacity flow rate of the working fluid in the phase change processes is very large, $C_{\rm c,min}$ equals C_w. The numbers of the heat transfer units of the corresponding sections are

$$\begin{aligned} {\rm NTU_I} &= UA_{\rm I}/C_{\rm I,min}, \quad (8) \\ {\rm NTU_{III}} &= UA_{\rm III}/C_{\rm III,min}, \quad (9) \\ {\rm NTU_c} &= UA_c/C_{\rm c,min}, \quad (10) \end{aligned}$$

where UA is the thermal conductance.

The temperature of the working fluid remains the same during the phase change processes,

$$T_5 = T_6, \quad (11)$$

$$T_2 = T_3. \quad (12)$$

For the isentropic process 1–2, we have

$$s_2 = s_1. \quad (13)$$

The latent heat of vaporization r in Eq. (2) is a single value function of the temperature, which can be determined according to the thermodynamic property tables for water and steam as[37]

$$r = f(T_5). \quad (14)$$

When $T_{\rm g,in}$, C_g, $T_{\rm en}$, C_w, c_v, c_l, $UA_{\rm I}$, $UA_{\rm III}$, UA_c, and m are prescribed, equations (1)–(14) can be solved and the heat flow rate $Q_{\rm I}$, $Q_{\rm II}$, $Q_{\rm III}$, and Q_c can be calculated. Then, the output power W can be obtained as

$$W = Q_{\rm I}+Q_{\rm II}+Q_{\rm III}-Q_c. \quad (15)$$

The exergy destruction rate of the whole system is the sum of the exergy destruction rate in all processes, which equals the product of the entropy generation rate and the environment temperature.[12] The exergy destruction minimization is the same as the entropy generation minimization, and we only give one of them in the results.[18,38] According to the entropy balance equation of the system, the entropy change rate is zero when the system is steady. Then, the entropy generation rate equals the net entropy flow rate out of the system, including the net entropy flow rate from the flue gas, the net entropy flow rate from the cooling water, and the entropy generation rate due to the heat released from the cycle to the environment. The cooling water is from the environment and exhausted to the environment after being heated, so the net entropy generation rate of the cooling water is zero. Therefore, the exergy destruction rate of the system is

$$\begin{aligned} I &= S_g T_{\rm en} = -S_f T_{\rm en} \\ &= \left(C_g \ln\frac{T_{\rm en}}{T_{\rm g,in}} + C_w \ln\frac{T_{\rm en}}{T_{\rm w,in}} \right. \\ &\quad \left. + \frac{C_g(T_{\rm g,in}-T_{\rm en}) + C_w(T_{\rm w,in}-T_{\rm en}) - W}{T_{\rm en}}\right) T_{\rm en} \\ &= C_g T_{\rm en} \ln\frac{T_{\rm en}}{T_{\rm g,in}} + C_g(T_{\rm g,in}-T_{\rm en}) - W. \quad (16) \end{aligned}$$

The entransy loss rate is defined as the entransy change in the thermodynamic processes due to heat transfer and heat-work conversion. It was found in many cases that the maximum entransy loss leads to the maximum output work.[27,33–35] The entransy loss rate of the system can be expressed as the difference of the entransy flow rate from the high temperature heat source $G_{\rm H}$ and that leaving the thermodynamic system $G_{\rm L}$. Similar to the entropy generation rate, the entransy flow rate contains three parts: the net entransy flow rate from the flue gas, the net entransy flow rate from the cooling water, and the entransy flow rate into the environment. The

entransy loss rate of the system is the difference between the entransy flow rate into the system and that out of the system

$$\begin{aligned} G_{\text{loss}} &= G_{\text{H}} - G_{\text{L}} \\ &= \frac{C_{\text{g}}\left(T_{\text{g,in}}^2 - T_{\text{en}}^2\right)}{2} + \frac{C_{\text{w}}\left(T_{\text{w,in}}^2 - T_{\text{en}}^2\right)}{2} \\ &\quad - \left[C_{\text{g}}\left(T_{\text{g,in}} - T_{\text{en}}\right) + C_{\text{w}}\left(T_{\text{w,in}} - T_{\text{en}}\right) - W\right] T_{\text{en}} \\ &= \frac{C_{\text{g}}\left(T_{\text{g,in}} - T_{\text{en}}\right)^2}{2} + W T_{\text{en}}. \end{aligned} \tag{17}$$

2.2. Numerical examples and discussion

Typical cases are discussed numerically below. In the first one, $T_{\text{g,in}} = 1800$ K, and $T_{\text{en}} = 298.15$ K. Some parameters are simplified to be constants, which are $c_{\text{l}} = 5 \times 10^3$ J/(kg·K), $c_{\text{v}} = 4 \times 10^3$ J/(kg·K), $C_{\text{g}} = 1.344 \times 10^6$ W/K, and $c_{\text{w}} = 4.2 \times 10^3$ J/(kg·K). The UA is the product of the heat transfer coefficient and the heat transfer area. We assume that $UA_{\text{I}} = 1.2 \times 10^6$ W/K, $UA_{\text{III}} = 7 \times 10^5$ W/K,[39] $UA_{\text{c}} = 1.5 \times 10^8$ W/K,[40] and the mass flow rate of the cooling water is 80 times of m.[1] The output power, exergy destruction rate, and entransy loss rate are calculated under different mass flow rates. The chosen parameters and the calculation results are close to a real 600-MW power plant.

The variations of the normalized output power, exergy destruction rate, and entransy loss rate with the mass flow rate are shown in Fig. 2. The scale of the output power, exergy destruction rate, and entransy loss rate are respectively from 618.29 MW to 622.39 MW, from 675.63 MW to 679.73 MW, and from 1.7001×10^{12} W·K to 1.7013×10^{12} W·K. The output power increases first as the mass flow rate increases, and then reduces because the efficiency of the cycle rapidly decreases due to the decrease in the evaporation temperature. The entransy loss rate also increases first and then decreases with increasing mass flow rate, while the exergy destruction rate decreases first and then increases. As the highest temperature and heat capacity flow rate of the flue gas are definite, the exergy input rate by flue gas is constant. It is known that a portion of the exergy input rate is lost in operating, and the rest is converted into output power. Thus, the trend of exergy destruction is opposite to the output power. According to Eq. (17), the entransy loss rate is proportional to the output power when C_{g} and $T_{\text{g,in}}$ are fixed. When m = 400.3 kg/s, the output power and entransy loss rate reach their maximum values, while the exergy destruction rate gets the minimum. The minimum exergy destruction rate and the maximum entransy loss rate both correspond to the maximum output power.

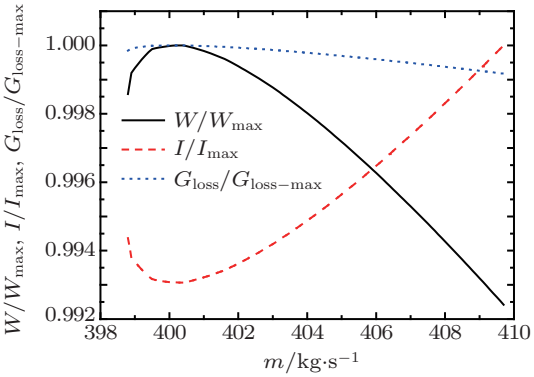


Fig. 2. (color online) Normalized output power, exergy destruction rate, and entransy loss rate under different mass flow rates of the basic Rankine cycle.

In the second case, we further discuss the variation of output power under different conditions, such as the variant heat capacity flow rate and flue gas temperature. Actually, the electric generation of power plants is not always maintained at a constant. For example, in order to modulate valley power, power plants often operate in low load conditions, under which the output heat and the relevant parameters of flue gas should be decreased. The variations of the output power with the highest temperature of the flue gas at a given mass flow rate $m = 400$ kg/s is discussed. We change the highest temperature of flue gas, and calculate the output power, exergy destruction rate, and entransy loss rate. The results are shown in Fig. 3. The scale of the output power, exergy destruction rate, and entransy loss rate are respectively from 594.38 MW to 623.78 MW, from 653.31 MW to 679.29 MW, and from 1.6035×10^{12} W·K to 1.7108×10^{12} W·K. Different from the first example, all the output power, exergy destruction rate, and entransy loss rate continuously increase with increasing the highest flue gas temperature. The increasing flue gas temperature causes the cycle efficiency to increase, and the output work increases in turn. However, according to the exergy method, the exergy destruction rate should decrease when the output power increases. The reason for the increase in exergy destruction rate is that the exergy input rate increases as the flue gas temperature and the total heat absorption rate of the system increase. The exergy destruction rate does not only depend on the perfectness of the cycle to a reversible one, but also on the total exergy input rate.

In the third case, we set the heat capacity flow rate of flue gas as a variable, and calculate the output power, exergy destruction rate, and entransy loss rate. The results are shown in Fig. 4. The scale of the output power, exergy destruction rate, and entransy loss rate are respectively from 605.39 MW to 623.25 MW, from 651.10 MW to 680.29 MW, and from 1.6477×10^{12} W·K to 1.7080×10^{12} W·K. Similar to Fig. 3, the output power, exergy destruction rate, and entransy loss rate all increase continuously with the heat capacity flow rates of the flue gas. Again, the minimum exergy destruction rate

does not lead to the maximum output power because of the input change in the total heat and exergy rate into the system.

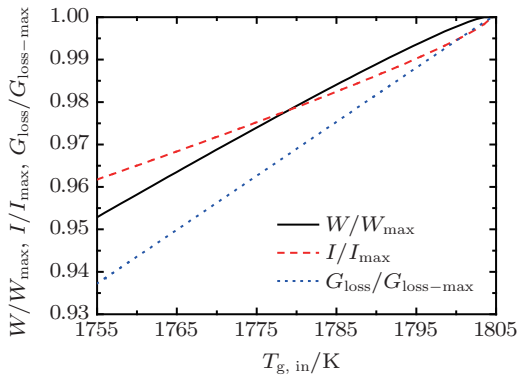


Fig. 3. (color online) Normalized output power, exergy destruction rate, and entransy loss rate under different highest flue gas temperatures of the basic Rankine cycle.

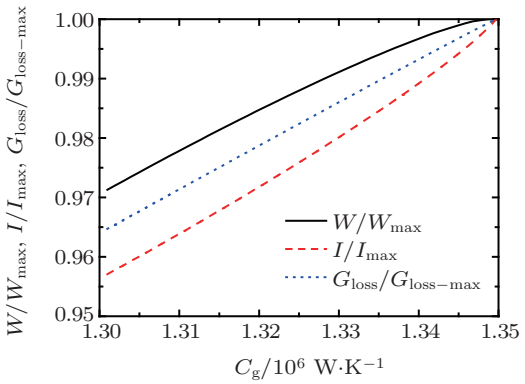


Fig. 4. (color online) Normalized output power, exergy destruction rate, and entransy loss rate under different heat capacity flow rates of flue gas.

The above discussion shows that the minimum exergy destruction and the maximum entransy loss can be used to optimize the output power from the basic Rankine cycle of the thermal power plants when the total heat and exergy input into the system is prescribed. If the exergy input is changed, larger exergy destruction and entransy loss correspond to larger output power.

3. Analyses of the Rankine cycle with a reheating process

3.1. Thermodynamic processes in thermal power plants with a reheater

In thermal power plants, reheating is usually applied to the basic Rankine cycle to raise the average temperature of heat absorption,[12] so that the cycle efficiency can be modified. Figure 5(a) is the sketch of the Rankine cycle in a thermal power plant with a reheater. The difference between the basic Rankine cycle and the present cycle is the reheating process. After the high-pressure superheated steam has done some work in the high-pressure turbines, it flows into the reheater and is heated again to a high temperature that is nearly the temperature of the initial superheated steam. Then the high-temperature steam flows to the low-pressure turbines and does work.

According to Fig. 5(a), the reheater is arranged between the superheater and the economizer in the flue loop. The T–s diagram of the system with a reheater is shown in Fig. 5(b). $T_{\rm g,in3}$ is the outlet temperature of the flue gas through the superheater, and also the inlet temperature of the flue gas into the reheater. $T_{\rm g,in4}$ is the outlet temperature of the flue gas through the reheater, and also the inlet temperature of the flue gas into the economizer. $T_{\rm B}$ is the temperature of the steam out of the high pressure turbines before the reheater inlet. $T_{\rm A}$ is the temperature of the steam out of the reheater before the low pressure turbines. Processes in the turbines are all isentropic.

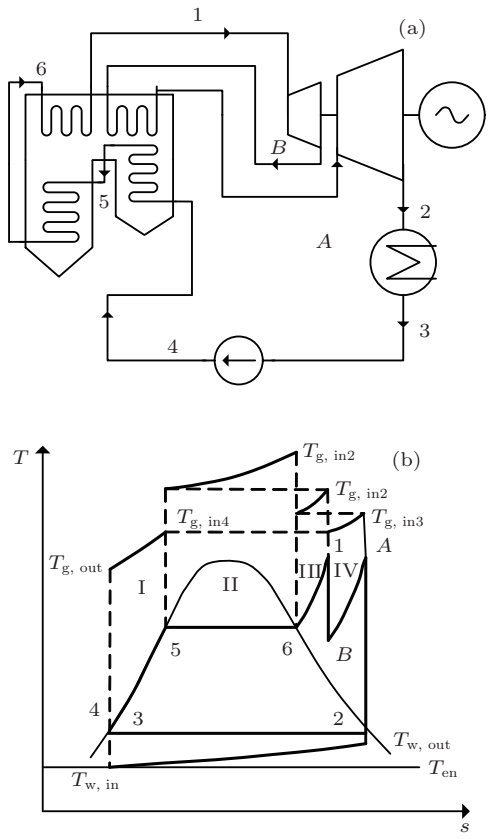


Fig. 5. (a) The flow diagram of the Rankine cycle with a reheating process. (b) The T–s diagram of the Rankine cycle with a reheating process.

Taking the maximum output power as the analyses objective, we can also solve the problem. The energy balance equations in sections I and IV are

$$\begin{aligned} Q_{\rm I} &= mc_{\rm l}\left(T_5 - T_3\right) = C_{\rm I,min}\varepsilon_{\rm I}\left(T_{\rm g,in4} - T_3\right) \\ &= C_{\rm g}\left(T_{\rm g,in4} - T_{\rm g,out}\right), \end{aligned} \tag{18}$$

$$\begin{aligned} Q_{\rm IV} &= mc_{\rm vr}\left(T_A - T_B\right) = C_{\rm IV,min}\varepsilon_{\rm IV}\left(T_{\rm g,in3} - T_B\right) \\ &= C_{\rm g}\left(T_{\rm g,in3} - T_{\rm g,in4}\right), \end{aligned} \tag{19}$$

where c_{vr} is the specific heat capacity of the reheated vapor under low pressure, and subscript IV indicates the corresponding parameters of the reheating section. The pressure of the reheated steam is lower than the initial steam, while the temperature is close to it.[1] We suppose that

$$T_A = T_1. \tag{20}$$

Process 1–B in the cycle is isentropic, so

$$s_1 = s_B. \tag{21}$$

The flow mode of the working fluid in the reheater is considered to be a counter flow,[1] and its effectiveness is

$$\varepsilon_{IV} = \frac{1-\exp\left[(-NTU_{IV})\left(1-C_{IV,min}/C_{IV,max}\right)\right]}{1-\left(C_{IV,min}/C_{IV,max}\right)\exp\left[(-NTU_{IV})\left(1-C_{IV,min}/C_{IV,max}\right)\right]}, \tag{22}$$

where $C_{IV,min}$ is the smaller one between C_g and mc_{vr}, and $C_{IV,max}$ is the larger one. NTU_{IV} is the number of transfer units of the reheating heat exchanger

$$NTU_{IV} = UA_{IV}/C_{IV,min}, \tag{23}$$

where UA_{IV} is its thermal conductance.

We can solve Eqs. (2), (4)–(14), and (18)–(23) when $T_{g,in}$, C_g, T_{en}, C_w, c_v, c_l, c_{vr}, UA_I, UA_{III}, UA_{IV}, UA_c, and m are given. The output power W is the difference between the absorbed heat flow rates and the released heat flow rate by the working fluid

$$W = Q_I + Q_{II} + Q_{III} + Q_{IV} - Q_c. \tag{24}$$

The calculation of the exergy destruction rate and entransy loss rate is the same as Eqs. (16) and (17).

3.2. Results and discussion of the numerical examples with a reheater

We assume that $T_{g,in} = 1800$ K, $T_{en} = 298.15$ K, $C_g = 1.344\times10^6$ W/K, $c_l = 5\times10^3$ J/(kg·K), $c_v = 4\times10^3$ J/(kg·K), and $c_{vr} = 2.3\times10^3$ J/(kg·K) are simplified to be constants, $UA_I = 1\times10^6$ W/K, $UA_{III} = 5\times10^5$ W/K, $UA_{IV} = 3\times10^5$ W/K,[39] $UA_c = 1.5\times10^8$ W/K, and the mass flow rate of cooling water is 80 times of m. The output power, exergy destruction rate, and entransy loss rate are calculated under different mass flow rates. The scale of the data and results nearly match a real 600-MW power plant. In this calculation, a lower steam mass flow rate is needed in the reheat cycle than that in the basic Rankine cycle. The scale of the output power, exergy destruction rate, and entransy loss rate are respectively from 605.13 MW to 613.12 MW, from 684.91 MW to 692.90 MW, and from 1.6962×10^{12} W·K to 1.6985×10^{12} W·K. When the mass flow rate increases, our numerical results show that the variation tendencies of the output power, the entransy loss rate, and the exergy destruction rate are the same as those in Fig. 2. When $m = 346.8$ kg/s, the normalized output power and entransy loss rate reach their maximum, while the exergy destruction rate reaches its minimum. It means that once the heat capacity flow rates and the inlet temperature of the flue gas are prescribed, both the minimum exergy destruction rate and the maximum entransy loss rate can be used to optimize the Rankine cycle with a reheating process by taking the maximum output work as the objective.

The highest temperature of the flue gas is changed to demonstrate its effect on the output power for a fixed mass flow rate of 350 kg/s. When $T_{g,in}$ increases, our numerical results show that the variation tendencies of the output power, exergy destruction rate and entransy loss rate are the same as those in Fig. 3. The scale of the output power, exergy destruction rate, and entransy loss rate are respectively from 584.57 MW to 625.13 MW, from 660.89 MW to 704.34 MW, and from 1.5966×10^{12} W·K to 1.7592×10^{12} W·K. The highest flue gas temperatures are generally higher than those of the ideal Rankine cycle. Similar to Fig. 3, the output power, exergy destruction rate, and entransy loss rate increase continuously with increasing the highest temperature of the flue gas.

Furthermore, the variations of the output power, exergy destruction rate, and entransy loss rate with heat capacity flow rates of flue gas are also calculated, and the numerical results show that the variation tendencies of the discussed parameters are the same as those in Fig. 4. The scales of the output power, exergy destruction rate and entransy loss rate are respectively from 594.31 MW to 620.49 MW, from 655.04 MW to 709.99 MW, and from 1.6361×10^{12} W·K to 1.7386×10^{12} W·K. The heat capacity flow rates of flue gas are generally greater than those of the ideal Rankine cycle. The output power, exergy destruction rate, and entransy loss rate increase continuously with increasing heat capacity flow rates of the flue gas.

The results of the Rankine cycle with a reheater shows that both exergy destruction minimization and entransy loss maximization can be used to optimize output work when the flue gas temperature and heat capacity flow are prescribed. When the highest temperature or the heat capacity flow rates of flue gas are not determined, the minimum exergy destruction rate does not lead to the maximum output power, while the maximum entransy loss rate does.

4. Analyses of the Rankine cycle with a regenerative process

4.1. Thermodynamic processes in the Rankine cycle with a single stage regeneration

Regeneration is also usually used to improve the heat-work conversion efficiency of low-temperature heat absorption. Parts of steam flows which have done some work are extracted under different pressures to heat the feed water in the regenerative heater and to reduce its heat absorption from the boiler.[12] A single stage steam extraction regeneration, for example, is illustrated in Fig. 6(a). A part of the vapor at state 0 is extracted to the regenerative heater. The extracted fraction is α and other parts, 1–α, continue to do work to complete the Rankine cycle, and then flow into the regenerative heater as well. The two parts directly mix in the regenerative heater, change into state 0′, and flow into the boiler to absorb heat. The other processes of the cycle are the same as those of the basic Rankine cycle.

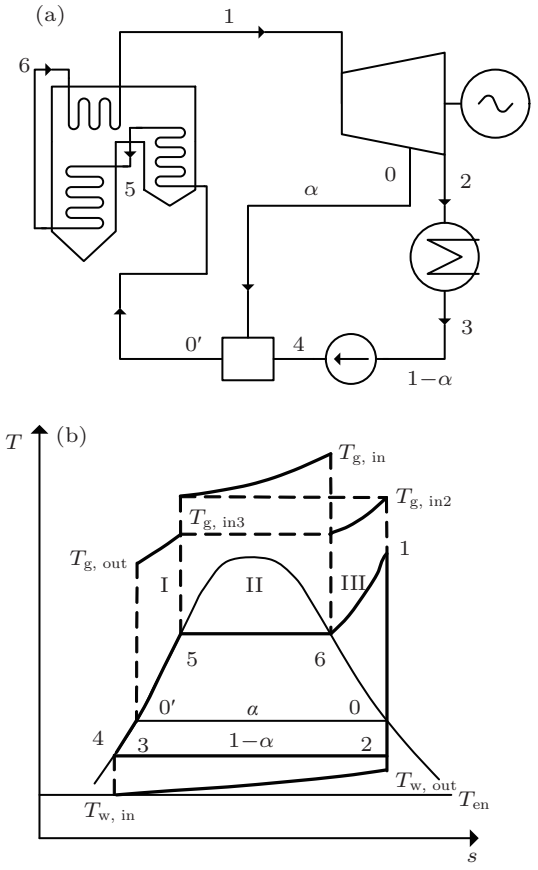


Fig. 6. (a) The sketch of the Rankine cycle with a single stage steam extraction regenerative process. (b) The T–s diagram of the Rankine cycle with a single stage steam extraction regenerative process.

According to Fig. 6(b), it is assumed that the status of the extracted steam is saturated vapor or wet steam. The heat balance in the economizer, regenerative heater and condenser are

$$\begin{aligned} Q_{\mathrm{I}} &= mc_{\mathrm{l}}\left(T_5 - T_{0'}\right) = C_{\mathrm{I,min\,1}}\varepsilon_{\mathrm{I}}\left(T_{\mathrm{g,in3}} - T_{0'}\right) \\ &= C_{\mathrm{g}}\left(T_{\mathrm{g,in3}} - T_{\mathrm{g,out}}\right), \end{aligned} \tag{25}$$

$$Q_{\mathrm{r}} = \alpha T_0(s_0 - s_{0'}) = (1-\alpha)mc_{\mathrm{lr}}(T_{0'} - T_3), \tag{26}$$

$$\begin{aligned} Q_{\mathrm{c}} &= C_{\mathrm{c,min}}\varepsilon_{\mathrm{c}}(T_2 - T_{\mathrm{w,in}}) = C_{\mathrm{w}}(T_{\mathrm{w,out}} - T_{\mathrm{w,in}}) \\ &= (1-\alpha)mT_2(s_2 - s_3), \end{aligned} \tag{27}$$

where c_{lr} is the specific heat capacity of the low pressure water at constant pressure in the regenerative heater. Process 0–0′ of extracted steams in the regenerative heater changes in phase, so

$$T_0 = T_{0'}. \tag{28}$$

Process 1–0 for the extracted steam is isentropic, thus

$$s_0 = s_1. \tag{29}$$

The other equations are the same as the basic Rankine cycle. Based on Eqs. (2), (3), (5)–(14), and (25)–(29), the whole system can be solved. The output power, exergy destruction rate, and entransy loss can be calculated by Eqs. (15)–(17).

4.2. Results and discussion of the numerical examples

We assume that $T_{\mathrm{g,in}} = 1800$ K, $T_{\mathrm{en}} = 298.15$ K, $c_{\mathrm{l}} = 5 \times 10^3$ J/(kg·K), $c_{\mathrm{v}} = 4 \times 10^3$ J/(kg·K), $c_{\mathrm{lr}} = 4.2 \times 10^3$ J/(kg·K), $C_{\mathrm{g}} = 1.344 \times 10^6$ W/K, $c_{\mathrm{w}} = 4.2 \times 10^3$ J/(kg·K) are simplified to be constants, $UA_{\mathrm{I}} = 1.0 \times 10^6$ W/K, $UA_{\mathrm{III}} = 8 \times 10^5$ W/K, $UA_{\mathrm{c}} = 1.5 \times 10^8$ W/K, and the mass flow rate of cooling water is 80 times of m. The steam extraction coefficient α is 0.2. These values are also close to a 600-MW power plant.

Our numerical results show that the variation tendencies of the output power, exergy destruction rate, and entransy loss rate under different mass flow rates are also the same as those in Fig. 2. The scale of the output power, exergy destruction rate and entransy loss rate are respectively from 595.06 MW to 602.28 MW, from 695.75 MW to 702.97 MW, and from 1.6931×10^{12} W·K to 1.6953×10^{12} W·K. The results are similar to those of the above sections, while higher steam mass flow rate is needed. We also found that both the exergy destruction minimization and the maximum principle of entransy loss can be used to optimize the Rankine cycle with a single stage steam extraction regenerative process for the maximum output work.

The mass flow rate is set at 480 kg/s, and the highest inlet temperature of the flue gas is changed in the following case. Our numerical results also show that the variation tendencies of the output power, exergy destruction rate, and entransy loss rate are the same as those in Fig. 3, while the scale of the output power, exergy destruction rate, and entransy loss rate are respectively from 544.30 MW to 619.72 MW, from 636.69 MW to 728.89 MW, and from 1.4735×10^{12} W·K to 1.7927×10^{12} W·K. For the case where the fixed parameter is not the heat capacity flow rates but the inlet temperature of flue

gas, our numerical results also show that the output power, exergy destruction rate, and entransy loss rate all increase continuously when the heat capacity flow rates of the flue gas increase, and the scale of the output power, exergy destruction rate, and entransy loss rate are respectively from 562.88 MW to 614.10 MW, from 631.30 MW to 742.34 MW, and from 1.5623×10^{12} W·K to 1.7670×10^{12} W·K.

5. Conclusions

Taking the maximum output power of thermal power plants as the objective, we analyze three kinds of thermal power plants by exergy destruction and entransy loss. The first one consists of a steam Rankine cycle, flue gas in a combustion chamber, and cooling water; the second one is a variation of the first one in which a reheating process is added to the Rankine cycle; and the third one is also a variation of the first one in which a regenerative extraction process is added. The latter two cases are analyzed by entransy loss for the first time. The correspondence between the output power and the cycle mass flow rate, the highest temperature or heat capacity flow rate of the flue gas are analyzed. It is found that the minimum exergy destruction rate and the maximum entransy loss rate both correspond to the maximum output power in the present calculation scale and cases when the highest temperature and heat capacity flow rates of the flue gas are prescribed. However, under the conditions of variant highest temperature and heat capacity flow rate of the flue gas, larger entransy loss rate leads to larger output power, but smaller exergy destruction rate does not.

References

[1] Nag P K 2002 *Power Plant Engineering* (2nd Edn.) (New Delhi: McGraw-Hill)

[2] Vundela S R, Subhash C K, Sudhir K T and Naraya L P 2010 *Smart Grid and Renewable Energy* **1** 143

[3] Ibrahim D and Husain A 2001 *Int. J. Energ. Res.* **25** 727

[4] Habib M A and Zubair S M 1992 *Energy* **3** 295

[5] Bo L, Philippe R, Christophe C, Renaud G and Franck D 2012 *Appl. Energ.* **100** 285

[6] Chen L G, Wu C and Sun F R 1999 *J. Non-Equilibrium Thermodynamics* **24** 327

[7] Chen L G and Sun F R 2004 *Advances in Finite Time Thermodynamics: Analysis and Optimization* (New York: Nova Science Publishers)

[8] Chen L G, Li J and Sun F R 2008 *Appl. Energ.* **85** 52

[9] Chen L G, Feng H J and Sun F R 2013 *J. Energ. Institute* **86** 97

[10] Kaushik S C, Reddy V S and Tyagi S K 2011 *Renew. Sust. Energ. Rev.* **15** 1857

[11] Li Q D and Liu Z Z 2008 *Thermal Economy Calculation and Analysis of Thermal Power Plant* (Beijing: China Electric Power Press) (in Chinese)

[12] Moran M J and Shapiro H N 2010 *Fundamentals of Engineering Thermodynamics* (6th Edn.) (New York: John Wiley & Sons)

[13] Adavbiele A S 2010 *Int. J. Eng. Res. Africa* **1** 67

[14] Li P, Gong M Q and Wu J F 2008 *J. Appl. Phys.* **104** 103536

[15] Myat A, Thu K and Kim Y D 2011 *Appl. Therm. Energ.* **31** 2405

[16] Cheng X T and Liang X G 2013 *Chin. Phys. B* **22** 010508

[17] Bejan A 1997 *Advanced Engineering Thermodynamics* (New York: John Wiley & Sons)

[18] Salamon P, Hoffmann K H, Schubert S, Berry R S and Andresen B 2001 *J. Non-Equilib. Thermodyn.* **26** 73

[19] Klein S A and Reindl D T 1998 *J. Energ. Res.* **120** 172

[20] Cheng X T, Wang W H and Liang X G 2012 *Chin. Sci. Bull.* **57** 2934

[21] Sengupta S, Datta A and Duttagupta S 2007 *Int. J. Eng. Res.* **31** 14

[22] Naterer G F, Regulagadda P and Dincer I 2010 *Appl. Therm. Energ.* **30** 970

[23] Habib M A, Said S A M and Al-Zaharna I 1999 *Appl. Energ.* **63** 17

[24] Acar H I 1997 *Energ. Convers. Manage* **38** 647

[25] Khaliq A and Kaushik S C 2002 *Appl. Eng.* **78** 179

[26] Guo Z Y, Zhu H Y and Liang X G 2007 *Int. J. Heat Mass Tran.* **50** 2545

[27] Chen L G 2012 *Chin. Sci. Bull.* **57** 4404

[28] Feng H J, Chen L G and Sun F G 2012 *Sci. China: Tech. Sci.* **55** 779

[29] Feng H J, Chen L G, Xie Z H and Sun F R 2013 *Sci. China: Tech. Sci.* **56** 299

[30] Cheng X T and Liang X G 2012 *Energy* **41** 964

[31] Cheng X T and Liang X G 2012 *Energy* **47** 421

[32] Cheng X T, Wang W H and Liang X G 2012 *Sci. China: Tech. Sci.* **55** 2847

[33] Zhou B, Cheng X T and Liang X G 2013 *Sci. China: Tech. Sci.* **56** 228

[34] Wang W H, Cheng X T and Liang X G 2013 *Energ. Convers. Manage.* **68** 82

[35] Zhou B, Cheng X T and Liang X G 2013 *J. Appl. Phys.* **113** 124904

[36] Holman J P 2001 *Heat Transfer* (8th Edn.) (New York: McGraw-Hill)

[37] Wagner W and Kruse A 1998 *Properties of Water and Steam: the Industrial Standard IAPWS-IF97 for the Thermodynamic Properties and Supplementary Equations for Other Properties: Tables Based on These Equations* (Berlin, New York: Springer-Verlag)

[38] Cheng X T and Liang X G 2013 *Energ. Convers. Manage.* **73** 121

[39] Lin Z H and Xu T M 2009 *Practical Boiler Manual* (2nd Edn.) (Beijing: Chemical Industry Press) (in Chinese)

[40] Zhang W G, Ye X M and Wu R T 2012 *Power System Engineering* **28** 59